doi:10.14311/ppt.2019.1.51

Plasma Physics and Technology **6**(1):51–55, 2019

MODELLING AND EXPERIMENTAL INVESTIGATIONS OF DC ELECTRIC ARCS IN ARGON AND CARBON DIOXIDE

C. Mohsni[a, b, *], M. Baeva[a], St. Franke[a], S. Gortschakow[a], D. Gonzalez[a], Z. Araoud[b], K. Charrada[b]

[a] *Leibniz Institute for Plasma Science and Technology, Felix-Hausdorff-Str. 2, 17489 Greifswald, Germany*

[b] *National School of Engineering of Monastir, 5000 Rue Ibn Jazzar, Monastir 5035, Tunisia*

[*] mohsni_chayma@hotmail.fr

Abstract. In this work an arc model is employed along with electric and spectroscopic measurements to study DC electric arcs in Ar and CO_2. The model is aimed at describing the arc and the electrodes. Simulation and experimental results are shown for currents between 150 A and 210 A.

Keywords: thermal plasma, electric arcs, plasma-electrode interaction, plasma diagnostics.

1. Introduction

Experimental and simulation studies of electric arcs, which are used in industrial applications, are important for a deeper understanding of the arc process. Some gases such as SF_6, used in circuit breakers, have a negative impact on the environment. Therefore, alternatives are considered and one potential candidate is carbon dioxide (CO_2) due to its electrical and chemical properties.

The modelling of electric arcs, which combines the equilibrium description of the bulk plasma and a non-equilibrium treatment of the near-electrode regions [1, 2], has been considered as an alternative to the fully equilibrium approach applied over the course of many years [3, 4] and the fully non-equilibrium approaches suggested more recently in [5, 6]. The combined modelling of the plasma bulk and the cathode boundary layer in DC arcs with a refractory cathode allows accounting for the significant amount of electric power deposited in the thin boundary layer adjacent to the cathode, in particular for currents below 200 A, and to reduce the discrepancy to the measured arc voltage, i.e. to improve the predictive capability of the model. This modelling approach can be, in general, more easily applied to molecular gases, which are used in industrial devices, e.g. circuit breakers.

In this work, DC arcs in argon and CO_2 were studied. A Local Thermodynamic Equilibrium (LTE) arc model in CO_2 was established while the model for argon is aimed at coupling the thermionic cathode, the LTE bulk plasma and the anode. To assess the model accuracy, electrical and spectroscopic measurements in various gases were carried out.

2. Model description

The development of the combined arc model includes two steps: the establishment of the LTE model of the arc column and the non-equilibrium model of the near-electrode regions. The LTE model is based on a magneto-hydrodynamic approach which involves the Navier-Stokes equations for conservation of mass, momentum and energy. The electrodes are included in the model and coupled to the plasma through a non-equilibrium boundary layer. It is assumed that the gas flow is laminar and the plasma behaves like a fluid which state is characterized by LTE. A stationary solution is sought for the equations

$$\nabla \cdot (\rho \mathbf{u}) = 0 \tag{1}$$

$$\rho(\mathbf{u} \cdot \nabla)\mathbf{u} = \nabla \cdot (-p\hat{I} + \hat{\tau}) + \mathbf{F_L} \tag{2}$$

$$\rho C_p(\mathbf{u} \cdot \nabla T) + \nabla \cdot \mathbf{q} = Q_\mathrm{J} - Q_\mathrm{rad} \tag{3}$$

where ρ is the mass density, $\mathbf{u}$ is the flow velocity, p is the pressure, $\hat{\tau}$ is the stress tensor, $\hat{I}$ is the identity matrix, and $\mathbf{F_L} = \mathbf{j} \times \mathbf{B}$ is the Lorentz force per unit volume. In Eq. (3), C_p is the specific heat at constant pressure, T is the gas temperature, $\mathbf{q} = -\kappa\nabla T$ is the heat flux due to thermal conduction with κ being the thermal conductivity. The gas is heated by Joule heating $Q_\mathrm{J} = \mathbf{j} \cdot \mathbf{E}$, where j is the electric current density, and cooled by radiation Q_rad. The Maxwell equations and the Ohm's law are used to obtain the self-induced magnetic field $\mathbf{B}$ and the electric potential φ

$$\nabla \times \mathbf{B} = \mu_0 \mathbf{j}; \quad \mathbf{B} = \nabla \times \mathbf{A} \tag{4}$$

$$\nabla \cdot \mathbf{j} = 0; \quad \mathbf{j} = \sigma\mathbf{E} = -\sigma\nabla\varphi \tag{5}$$

The electric field $\mathbf{E}$ and the magnetic field $\mathbf{B}$ couple the electromagnetic part of the model to the fluid through the Lorentz force per unit volume and the Joule heating. In Eq. (4) and (5), $\mathbf{A}$ is the vector potential and σ is the electrical conductivity. The transport properties were provided by A. B. Murphy as calculated according to [7, 8] and applying a C-C collision integral from [9].

The heat conduction and current continuity equations are solved in the electrodes:

$$\nabla \cdot (k_\mathrm{s}\nabla T) + \mathbf{j} \cdot \mathbf{E} = 0 \tag{6}$$

$$\nabla \cdot \mathbf{j} = 0 \; ; \quad \mathbf{j} = \sigma_s \mathbf{E} = -\sigma_s \nabla \varphi \tag{7}$$

The electrical conductivity σ_s and the thermal conductivity k_s of the solid materials are taken as a function of the temperature T. The cathode boundary layer includes the region of space-charge adjacent to the cathode surface (the sheath) and the ionization layer.

The energy balance in the boundary layer [10, 11] accounts for 1) the heat flux leaving the boundary layer and going to the cathode, 2) the electric power density deposited in the boundary layer, 3) the power brought by the electrons emitted from the cathode, and 4) the heat flux entering the boundary layer from the LTE plasma. The energy balance and the total current density, which is the sum of the density of the thermionic emission current (j_{em}), the ion current density (j_{ion}), and the current density transported by counter-diffusing electrons (j_{be}), determine the heat flux q_w and the current density j_w on the cathode surface as functions of the voltage drop U_{tot} in the boundary layer and the surface temperature T_w:

$$q_w(T_w, U_{tot}) = j_w U_{tot} - \frac{j_w}{e}(A_w - \Delta A_w + 3.2kT_e) \tag{8}$$

$$j_w\ (T_w, U_{tot}) = j_{em} + j_{ion} - j_{be} \tag{9}$$

Here, A_w is the work function of the electrode material, ΔA_w is the Shottky correction, T_e is the electron temperature obtained from the boundary layer model. The voltage drop in the near-cathode layer includes the voltage drop in the space-charge sheath (U_d) and that in the ionization layer (U_i), i.e. $U_{tot} = U_d + U_i$. A similar approach has been applied in [12].

Losses due to black-body radiation of the hot body are considered as $q_{rad} = \epsilon\sigma_{SB}T_w^4$. The resultant heat flux $q_c = q_w(T_w, U_{tot}) - q_{rad}$, and the current density $j_w(T_w, U_{tot})$ serve as boundary conditions of equations (6) and (7). The cathode boundary layer is solved prior to the arc simulation for a series of values of the temperature on the cathode boundary T_w and the voltage drop U_{tot}. The results are provided as lookup tables and are used during the iterative solution of the combined model.

The consideration of the plasma-anode boundary layer is simpler [13]. The expression for the heat flux as in many LTE models [3, 4] is used. The normal component of the energy flux to the surface q_a, which is added to the conductive one, is given by

$$q_a = -\epsilon\sigma_{SB}T_w^4 + |j_e|\, A_{an} \tag{10}$$

Here, ϵ is the emissivity of the surface, σ_{SB} is the Stefan-Boltzmann constant, j_e is the electron component of the current density and A_{an} is the work function of the anode material. The term $|j_e|A_{an}$ accounts for heating of the anode due to condensation of electrons. For pure tungsten, the work function and the Richardson constant are 4.55 eV and $0.602 \cdot 10^6$ Am^{-2}K^{-2}, respectively. The corresponding values for graphite are 4.6 eV and $0.600 \cdot 10^6$ Am^{-2}K^{-2}. The model is set up on the commercial computational platform COMSOL Multiphysics® using the interfaces Laminar flow, Electric current, Magnetic field and Heat transfer. The computational domain includes both electrodes and the inter-electrode space in a radial extend of 30 mm. A part of this domain is shown in Figure 1. Temperature of 300 K, electric and magnetic insulation are set on the external boundaries. The anode is grounded. The total arc voltage drop in the boundary layer is adjusted until the integral of the current density along the cathode surface equals the desired arc current.

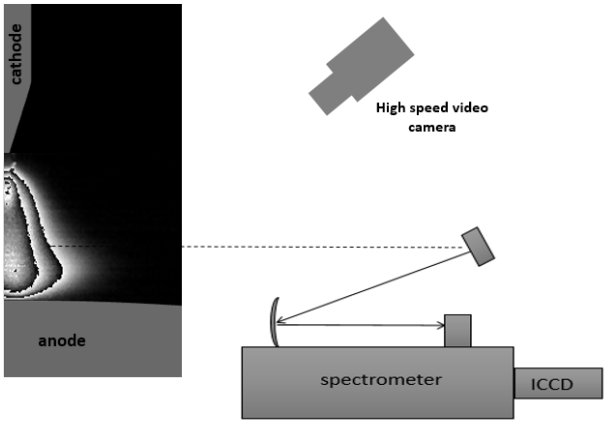

Figure 1. A view of the computational domain and the OES arrangement used for investigation of the arc.

3. Experimental setup

A view of the spectroscopic equipment and the computational domain is shown in Figure 1. The setup is tested for arcs in argon and CO_2. It comprises a spherically shaped anode, made of graphite and a cylindrical rod with a conical shape made of pure tungsten as cathode. The distance between the cathode tip and the anode is varied between 2 and 10 mm.

The image of the arc is taken by a high-speed video camera of the type IDT Motion Pro Y6. The arrangement is placed inside a chamber which is filled with gas up to the desired pressure. The latter is controlled by a manometer. The arc is ignited making use of a spark coil arrangement. The equipment for optical emission spectroscopy (OES) consists of a spectrograph Acton SP2500 with a focal length of 0.5 m and an intensified CCD camera Princeton Instruments PI-MAX4. Obtained images contain spectral and spatial side-on information about the arc. The arc is imaged by a spherical mirror on the entrance slit of the spectrometer with a width of 30 µm. Absolute calibration is performed by a tungsten strip lamp placed at the position of the arc.

The radiation of the Ar II line at 480 nm is spectrally resolved using a grating with 1800 lines/mm. The radiation of the O I line at 777 nm is resolved using a grating with 150 lines/mm. An integration over the wavelength range is performed and Abel inversion is done in order to get the radial dependence

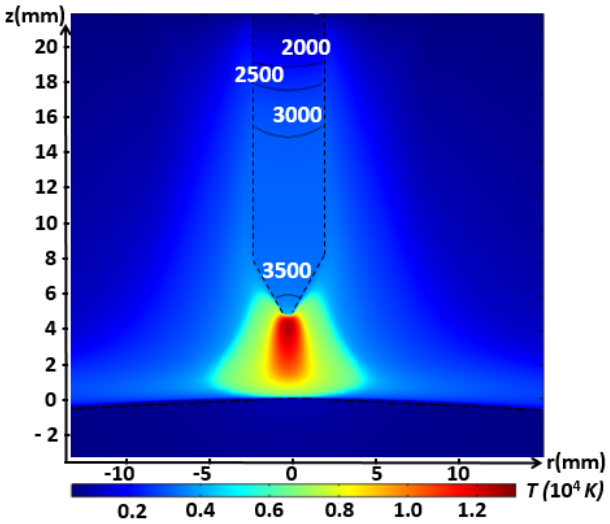

Figure 2. Two-dimensional distribution of the plasma temperature and the temperature in the electrodes obtained with the LTE model for an arc in CO_2 at current of 200 A.

of the emission coefficient. The number densities of the upper level corresponding to the transition of the Ar II 480 nm, O I 777 lines are derived assuming LTE. The population density is related to the plasma temperature. The temperature is obtained from a pre-calculated equilibrium composition of argon and carbon dioxide.

4. Results and discussion

Calculations with the LTE arc model were performed for the arrangement shown in Figure 1 with CO_2 at atmospheric pressure as working gas. Figure 2 shows the distribution of the temperature in the plasma and the electrodes for an arc current of 200 A. Since a matching of the boundary layer with the LTE plasma is not considered, the temperature in the arc seems to

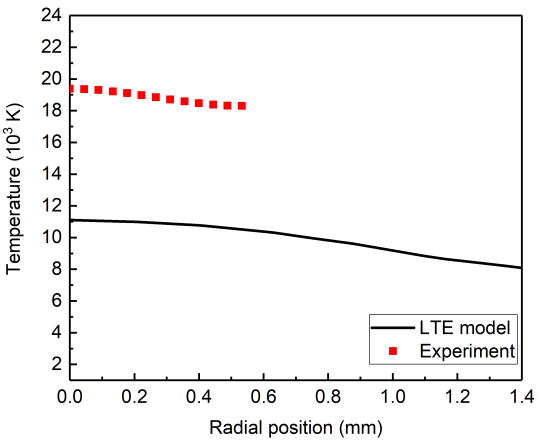

Figure 3. Radial plasma temperature obtained in the LTE model for an arc in CO_2 and the plasma temperature from OES for an arc current of 200 A at axial position 1 mm away from the cathode tip.

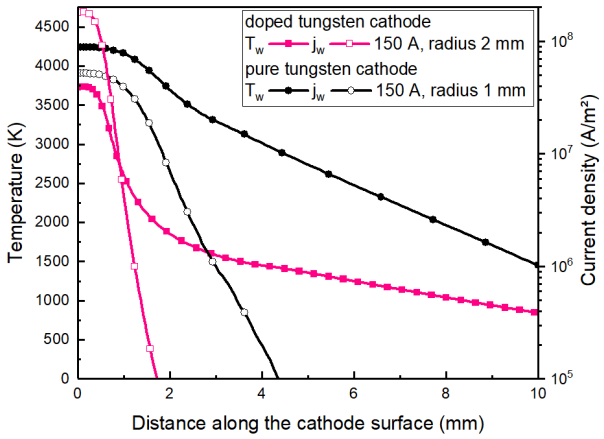

Figure 4. Temperature and normal current density along cathode surface for doped and pure tungsten cathodes for an arc current of 150 A.

be underestimated as the experimental results show in Figure 3.

The combined model has been applied first for argon as working gas to obtain the plasma parameters for arc currents of 150 A and 210 A. Figure 4 shows the temperature on the cathode surface and the current density for an arc current of 150 A for two cathode configurations: a) doped tungsten cathode (Ce-W) with a radius of 2 mm, and b) pure tungsten cathode with a radius of 1 mm. The profile of the temperature is more broadened and the arc attachment area is larger for the thinner electrode.

Melting of the electrodes and metal vapour are not considered in the model, which leads to temperatures higher than the melting point of tungsten. The normal current density at the cathode tip is 10% higher in the case of doped tungsten instead of pure tungsten. Figure 5 presents the components of the heat fluxes from the boundary layer to the cathode along the cathode surface for an arc current of 150 A. The

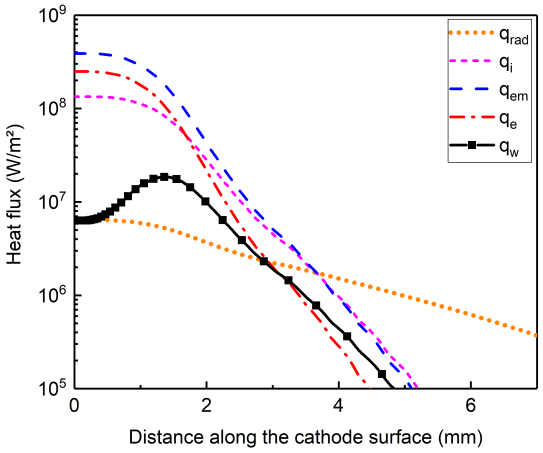

Figure 5. Total heat flux from the plasma to the cathode surface, its components and the contribution of the black body radiation along the cathode for an arc current of 150 A.

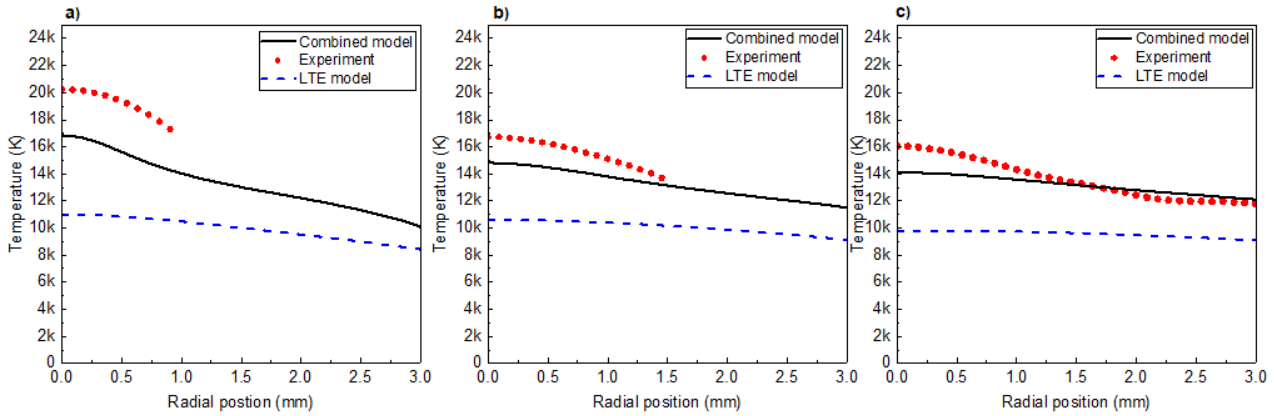

Figure 6. Temperature predicted by the combined model, LTE model and plasma temperature from optical emission spectroscopy at axial position 1mm a), 2.5 mm b) and 4 mm c) below the cathode. Arc current is 210 A.

solution shows that the dominant contribution at the cathode tip is that of the emitted electrons q_{em}, which exceeds those of the back diffusion electrons q_{e} and ions q_{i} contributions. From the position of 2 mm on, the main contributions are those of ions and emitted electrons. The resulting flux q_{w} around the cathode tip is lower than the other components, but still exceeds the contribution of the black body radiation q_{rad}.

The temperature predicted by the combined model in comparison with the LTE model and the values obtained from OES are shown in Figure 6. The results are presented for an arc current of 210 A and an arc length of 5 mm at three axial positions: 1 mm, 2.5 mm, and 4 mm away from the cathode tip. One can see that the radial distribution obtained by means of the combined model results in a more focused arc and in higher plasma temperatures near the cathode tip. This modelling approach provides a better agreement with the data obtained by emission spectroscopy.

5. Conclusions

The LTE model of the arc plasma is coupled with a model of the cathode boundary layer and is applied to an atmospheric pressure arc in argon. The consideration of the cathode boundary layer allows a more realistic description of the heat and current transfer in the electrodes and the plasma. Therefore, a similar approach has to be applied for CO_2. The model results are compared with experimental values and reasonable agreement is obtained.

Acknowledgements

Financial support of the German Academic Exchange Service (DAAD) is highly acknowledged (Grant No. 91644228).

References

[1] A. Shirvan et al. Effect of cathode model on arc attachment for short high-intensity arc on a refractory cathode. *J. Phys. D: Appl. Phys.*, 49(48):5201, 2016. doi:10.1088/0022-3727/49/48/485201/meta.

[2] M. Lisnyak et al. Numerical modelling of high-pressure arc discharges: matching the LTE arc core with the electrodes. *J. Phys. D: Appl. Phys.*, 50(31):5203, 2017. doi:10.1088/1361-6463/aa76d3/meta.

[3] J. J. Lowke et al. A simplified unified theory of arcs and their electrodes. *J. Phys. D: Appl. Phys.*, 30(14):2033–2042, 1997. doi:10.1088/0022-3727/30/14/011.

[4] L. Sansonnens et al. Prediction of properties of free burning arcs including effects of ambipolar diffusion. *J. Phys. D: Appl. Phys.*, 33(2):148–157, 2000. doi:10.1088/0022-3727/33/2/309.

[5] M. Baeva et al. Two-temperature chemically non-equilibrium modelling of transferred arcs. *Plasma Sources Science and Technology*, 21(5):5027, 2012. doi:10.1088/0963-0252/21/5/055027.

[6] M. Baeva et al. Novel non-equilibrium modelling of a DC electric arc in argon. *J. Phys. D: Appl. Phys.*, 49(24):5205, 2016. doi:10.1088/0022-3727/49/24/245205/meta.

[7] A. B. Murphy. Transport coefficients of air, argon-air, nitrogen-air, and oxygen-air plasmas. *Plasma Chem. Plasma Proc.*, 15(2):279, 1995. doi:10.1007/BF01459700.

[8] A. B. Murphy and C. J. Arundell. Transport-Coefficients of Argon, Nitrogen, Oxygen, Argon-Nitrogen, and Argon-Oxygen Plasmas. *Plasma Chem. Plasma Proc.*, 14(4):451–490, 1994. doi:10.1007/BF01570207.

[9] J. R. Stallcop at al. Potential energies and collision integrals for interactions of carbon and nitrogen atom. *J. Thermophys. Heat Transf.*, 14:480–488, 2000. doi:10.2514/2.6570.

[10] M. S. Benilov and A. Marotta. A Model of the Cathode Region of Atmospheric-Pressure Arcs. *J. Phys. D: Appl. Phys.*, 28(9):1869–1882, 1995. doi:10.1088/0022-3727/28/9/015/meta.

[11] M. S. Benilov and M. D. Cunha. Heating of refractory cathodes by high-pressure arc plasmas: I. *J. Phys. D: Appl. Phys.*, 35(14):1736–1750, 2002. doi:10.1088/0022-3727/35/14/314.

[12] S. Lichtenberg et al. The plasma boundary layer of HID-cathodes: modelling and numerical results. *J. Phys. D: Appl. Phys.*, 38(17):3112–3127, 2005. doi:10.1088/0022-3727/38/17/S13.

[13] J. Heberlein et al. The anode region of electric arcs: a survey. *J. Phys. D: Appl. Phys.*, 43(2):3001, 2010. doi:10.1088/0022-3727/43/2/023001/meta.